Carbohydrate-derived surfactants containing an N-Acylated amine functionality

Pestman, Jolanda Monique

Chapter 3

Aggregation Behavior of *N*-Acyl,*N*-alkyl-β-D-aldosylamines and *N*-Acyl,*N*-alkyl-1-amino-1-deoxy-D-alditols

3.1 Introduction

Lyotropic mesophases of the carbohydrate-derived surfactants described in chapter 2 were examined both at 40°C, at which the critical micelle concentrations were determined, and at ambient temperature. The characteristics of the mesophases indicate the shape of micelles formed in dilute solution.

The critical micelle concentrations were determined by two different techniques: drop tensiometry and titration rnicrocalorimetry. From plots of the surface tension vs surfactant concentration, the surface tensions at the CMC were determined and the headgroup areas of the surfactant molecules at the air-water interface were calculated from the slope of the curve below the CMC.

Titration rnicrocalorimetry provided, in addition to the critical micelle concentrations, the standard enthalpy of micellization, $\Delta_{mic}H°$. The standard Gibbs energies of micellization were calculated from the CMC, and thus the standard entropies of micellization could also be determined. The increments in standard enthalpies, Gibbs energies, and entropies of micellization per CH, for each series at 40°C offer important insights into the relationship between surfactant structure and the thermodynamic parameters describing aggregation."

3.2 Lyotropic liquid crystalline behavior

Surfactants adsorb strongly at air-water interfaces and at oil-water interfaces, reducing the surface tension and the interfacial tension, respectively. When added to water, surfactants start to aggregate at a certain concentration (the critical micelle concentration, see also Chapter 1). Above the CMC, added surfactant leads to an increase in the concentration of micelles. At substantially higher concentrations, there is a disorder/order transition with the formation of lyotropic liquid crystals (mesophases).[1]

Four well established mesophases are: lamellar, (inverted) hexagonal, cubic, and nematic (Figure 1). The lamellar phase (L_α) consists of surfactant bilayers separated by water layers. The hexagonal phase (H,) consists of elongated micelles with circular cross sections. The headgroups reside at the micellar surface with a continuous water region separating adjacent

[a] These derived thermodynamic parameters describe the formation of micelles by a mole of monomer.

micelles (Figure 1). One class of cubic mesophase (I,)can be found at compositions between the micellar solution and the hexagonal phase. This phase comprises closely packed cubical arrays of small globular micelles. A second type of cubic phase (V,), found at compositions between hexagonal and lamellar phases, consists of a three-dimensional bicontinuous network with both surfactant and water forming continuous zones. Both types of cubic phases are optically isotropic.[2] Nematic phases, found between the micellar solution and either the hexagonal or lamellar phase, consist of cylindrical micelles or ordered small disc micelles.' We do not discuss a more detailed classification of the different mesophases.'

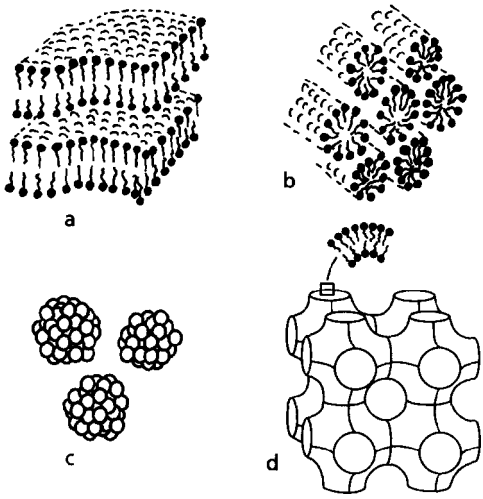

Figure 1. Some lyotropic mesophases: lamellar (L„ a), hexagonal (b), and two cubic phases (I,: c and V,: d).

The shape of the aggregates in solution can be rationalized on the basis of the packing parameter (Chapter 1).[3,4] The packing parameter identifies the optimal cross-sectional surface area per molecule (a„) for a particular shape of aggregate. For surfactants having alkyl chains with 8 - 12 carbon atoms, spheres are formed when $a_{\text{„}} > 63$ Å^2, rods are formed if 42 Å^2 < a_0 < 63 Å^2, bilayers if 21 Å^2 < a_0 < 42 Å^2 and inverted structures are formed if $a_{\text{„}} < 21$ Å^2.[5] Entropy favors the smallest possible micellar size and thus rods occur at a„ values smaller than the a„ values for a sphere, etc.[1]

The mesophase formed at the boundary of the micellar solution (the mesophase with the lowest surfactant concentration) provides an indication of the shape of the micelles in solution. An I, phase indicates spherical micelles, a hexagonal phase indicates rod-like rnicelles and a lamellar phase indicates either that the micelles in solution are disc-shaped or that vesicular aggregates are present in dilute solution. Further increases in surfactant

concentration lead to a continuing reduction of the surface area per molecule at the micelle surface. Therefore the expected mesophase transitions are:'

$$I_1 \rightarrow H_1 \rightarrow V_1 \rightarrow \text{lamellar } (L_\alpha)$$

Inverted phases will not be discussed, because these require relatively large hydrophobic tails and small hydrophilic headgroups.

Mesophases can be studied in various ways, including using the penetration technique. Pure surfactant is sandwiched between a microscope slide and a cover slip. The surfactant is melted and allowed to cool and, if possible, crystallize again. This process gives a well-defined surfactant boundary. The surfactant is then brought into contact with water. In these experiments, the whole concentration range from pure water to pure surfactant is covered.[6] Mesophases develop in concentric bands with characteristic optical textures which can be identified using a polarizing microscope.' The temperature dependence of the mesophase formation can be studied conveniently with the aid of a hot stage.'

3.2.1 Lyotropic mesophases formed by the carbohydrate-derived surfactants

To study the different lyotropic phases formed at ambient temperature and at 40°C, we performed penetration experiments at both temperatures; Table 1. The observations made at ambient temperature and at 40°C are similar in most cases. We did not investigate the nature of the optically isotropic phases further. For convenience, all optically isotropic phases are denoted as "cubic". This is an oversimplification, because not all optically isotropic phases are necessarily cubic.

The mesophase first encountered (*i.e.*, at the highest water concentration) is either a H_1 phase or a cubic phase. This result indicates the formation in solution of rods or spherical micelles, respectively. For most glucose- and glucitol-derived surfactants rod-shaped micelles are formed. The cubic phase formed from NC_3nC_{12} glucose is probably a V_1 phase, since the total number of alkyl carbons is too large to allow the formation of a hexagonal phase with the glucopyranoside headgroup. Propionylated glucitol-derived surfactants have higher Krafft temperatures than the acetylated ones. When mesophases did form in the contact experiments, they did not provide unambiguous clues as to the nature of the aggregates in dilute solution.

Table 1. Lyotropic mesophases of the glucose-, glucitol-, lactose- and lactitol-derived surfactants at ambient temperature and at 40°C.

Compound	lyotropic mesophases at ambient temperature	lyotropic mesophases at 40°C
NC_2nC_8 glucose	water-hex-bulk (isotropic)	water-hex-bulk (isotropic)
NC_2nC_{10} glucose	water-hex-bulk (viscous isotropic)	water-hex-bulk (viscous isotropic)
NC_2nC_{12} glucose	water-hex-cub-bulk (viscous isotropic)	water-hex-cub-bulk (viscous isotropic)
NC_3nC_8 glucose	water is absorbed without mesophases	water is absorbed without mesophases
NC_3nC_{10} glucose	water-hex-cub-bulk (viscous isotropic)	water-cub-bulk (viscous isotropic)
NC_3nC_{12} glucose	watercub-cub-L_a-bulk (S_A)	water-cub-cub-L,-bulk (S_A)
NC_2nC_8 glucitol	water-hex-cub-bulk (viscous isotropic)	water-hex-cub-bulk (viscous isotropic)
NC_2nC_{10} glucitol	water-hex-cub-L_a-bulk (S_A)	water-hex-cub-L_a-bulk (S_A)
NC_2nC_{12} glucitol	water-hex-cub-bulk (solid)	water-hex-cub-bulk (solid)
NC_3nC_8 glucitol	water is absorbed without mesophases	water is absorbed without mesophases
NC_3nC_{10} glucitol	T_{krafft} = 28°C[a]	water-hydrated bulk-bulk (solid)
NC_3nC_{12} glucitol	T_{Krafft} = 48°C	T_{Krafft} = 48°C[b]
NC_2nC_8 lactose	water-cub-hex-bulk (glass-like)	water-hex-bulk (glass-like)
NC_2nC_{10} lactose	water-cub-cub-hex-bulk (glass-like, S_A)[c]	water-cub-cub-hex-bulk (glass-like, S_A)[c]
NC_2nC_{12} lactose	water-cub-cub-hex-bulk (S_A)	water-cub-cub-hex-bulk (S_A)
NC_3nC_8 lactose	water-hex-bulk (viscous isotropic)	water-hexcub-bulk (viscous isotropic)
NC_3nC_{10} lactose	water-hex-bulk (S_A)[c]	water-hex-cub-bulk (S_A)[c]
NC_3nC_{12} lactose	water-hex-bulk (S_A)	water-hex-cub-bulk (S_A)
NC_2nC_8 lactitol	water-cub-hex-bulk (solid)	water-cub-hex-bulk (solid)
NC_2nC_{10} lactitol	water-cub-cub-hex-bulk (S_A)	watercub-cub-hex-bulk (S_A)
NC_2nC_{12} lactitol	water-cub-cub-hex-bulk (S_A)	water-cub-cub-hex-bulk (S_A)
NC_3nC_8 lactitol	water-hex-bulk (glass-like)	water-hex-bulk (glass-like)
NC_3nC_{10} lactitol	water-cub-cub-hex-bulk (solid)	water-hex-bulk (solid)
NC_3nC_{12} lactitol	water-hex-bulk (S_A)	water-hexcub-bulk (S_A)

[a] The Krafft temperature (T_{Krafft}) is the temperature at which the solubility of the surfactant equals the CMC. The solubility of surfactants increases dramatically above T_{Krafft}. [8] [b] At 50°C: water-cub-L_α-hydrated bulk-bulk (solid). 'Although this compound does not show a clearing point in the DSC (Chapter 2), it can crystallize with an S_A-like texture.

Lactose- and lactitol-derived surfactants have larger headgroups than the monosaccharide-derived surfactants. Spherical micelles are formed by the acetylated lactose- and lactitol-derived surfactants,[9] whereas the propionylated surfactants most likely form rod-shaped micelles. This pattern demonstrates that a small change in the "lateral" substituent influences the morphology of micelles in solution. The NC_3nC_{10} lactitol appears to behave anomalously. From the mesophases observed, one would predict the formation of spherical micelles, whereas the corresponding C_8 and C_{12} derivatives form rod-shaped micelles.

3.3 Drop tensiometry

3.3.1 Critical micelle concentrations measured by drop tensiometry

Figure 2 is an example of the important plot involved in the determination of the CMC by drop tensiometry. Critical micelle concentrations were measured at 40 °C to preclude possible solubility problems. However, all carbohydrate-derived surfactants (except NC_3nC_{12} glucitol) dissolve in water at ambient temperature. Table 2 records the CMCs of the carbohydrate-derived surfactants measured by drop tensiometry at 40°C. The critical micelle concentrations have the same order of magnitude as generally observed for nonionic surfactants and a number of trends are identified. The CMCs decrease by a factor of ten when the alkyl chain length is increased by two methylene groups. This tenfold decrease in CMC is also observed for polyethoxylated surfactants,[10] N-alkanoyl-N-methyl-glucamides (MEGAs),[11] and other nonionic surfactants[12-14]

Propionylated surfactants have slightly lower CMCs than their acetylated counterparts, which is accounted for by the larger hydrophobic components.[15] Addition of a methylene group in the short acyl chain, however, has a smaller effect (factor 1.5 - 2) on the CMC than the addition of a methylene group in the long alkyl chain (factor $\sqrt{10}$).

Generally speaking, the length of the alkyl chain determines the order of magnitude of the CMC. The headgroup size (monosaccharide vs disaccharide), shape (cyclic, acyclic, or a combination) as well as the configuration of the hydroxyl groups have only a small influence on the CMC. Table 2 shows that in our case, the nature of the headgroup influences the CMC within the order of magnitude determined by the chain length.[16,17]

Glucose-derived surfactants have lower CMCs than the lactose-derived surfactants, due to the smaller hydrophilic headgroup and the consequently relatively larger hydrophobic part. Surfactants with a reduced saccharide headgroup have lower CMCs than those with an intact cyclic structure. Probably, the (hydrated) alditol headgroup is somewhat smaller, but volumes of appropriate hydrated carbohydrate-derived headgroups are not known. (The values for the headgroup areas at the air-water interfaces are in most cases smaller for the alditols than for

the aldoses as will be shown in the next section).

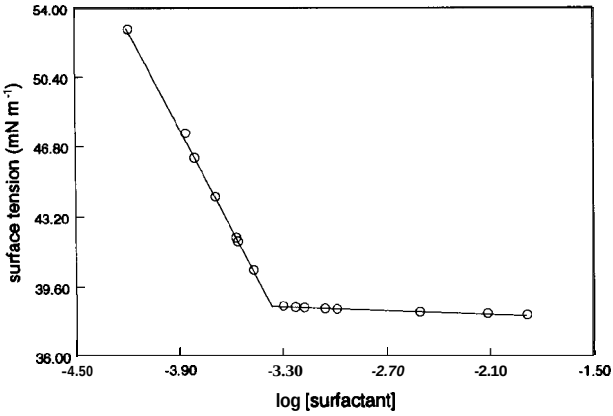

Figure 2. CMC determination of NC_2nC_{12} lactose by drop tensiometry.

Table 2. Critical micelle concentrations of the carbohydrate-derived surfactants measured by drop tensiometry at 40°C.[a]

compound	CMC (mM)	compound	CMC (mM)
NC_2nC_8 glucose[b]	25	NC_2nC_8 lactose[b]	40
NC_2nC_{10} glucose[b]	2.6	NC_2nC_{10} lactose[b]	3.4
NC_2nC_{12} glucose	0.31	NC_2nC_{12} lactose[b]	0.43
NC_3nC_8 glucose	18	NC_3nC_8 lactose	28
NC_3nC_{10} glucose	1.8	NC_3nC_{10} lactose	2.2
NC_3nC_{12} glucose	0.24	NC_3nC_{12} lactose	0.26
NC_2nC_8 glucitol	21	NC_2nC_8 lactitol	25
NC_2nC_{10} glucitol	1.9	NC_2nC_{10} lactitol	2.4
NC_2nC_{12} glucitol	0.20	NC_2nC_{12} lactitol	0.30
NC_3nC_8 glucitol	14	NC_3nC_8 lactitol	12
NC_3nC_{10} glucitol	1.1	NC_3nC_{10} lactitol	1.5
NC_3nC_{12} glucitol	0.13	NC_3nC_{12} lactitol	0.16

[a] The error in the measurements is about ± 2 in the last digit. [b] The CMCs of these surfactants have also been published by Rico-Lattes et *al.*,[18,19] the values are similar.

3.3.2 Surface tension at the CMC and headgroup area at the air-water interface

According to Table 3, the surface tension at the CMC decreases upon increasing chain lengths. Propionylated counterparts also display lower γ_{CMC} than the acetylated ones. Hence, the larger the hydrophobic part, the lower the surface tension at the CMC. This is not surprising. The interface becomes more alkane-like (*e.g.*, $\gamma = 25.4$ mN m^{-1} for dodecane).[14]

Surfactants with a glucitol headgroup seem to have slightly lower γ_{CMC} than the surfactants with a glucose headgroup. Both the monosaccharide-derived surfactants show much lower surface tensions at the CMC than the corresponding disaccharide-derived surfactants. Relatively high values for γ_{CMC} have also been observed for dodecyl β-D-maltose and for monododecyl esters of sucrose, raffinose, and stachyose.[5]

Lactose- and lactitol-derived surfactants show a similar reduction of the surface tension at the CMC (Table 3).

Table 3. Surface tension at the CMC of the carbohydrate-derived surfactants at 40°C (mN m^{-1})

	glucose	glucitol	lactose	lactitol
NC_2nC_8	35.6	35.0	43.4	42.9
NC_2nC_{10}	33.8	31.3	40.0	39.9
NC_2nC_{12}	30.6	30.3	38.5	39.4
NC_3nC_8	31.6	30.2	37.5	37.8
NC_3nC_{10}	29.3	29.3	34.1	37.1
NC_3nC_{12}	29.0	28.6	34.5	36.4

Table 4 records the area per molecule for each carbohydrate-derived surfactant at the air-water interface (&) at 40°C. These areas are calculated from the maximum surface excess concentration Γ:[20,21]

$$\Gamma = -(RT)^{-1} \cdot (d\gamma/d(\ln[\text{surfactant}]) = (N_{AV}A_0)^{-1} = -(2.303RT)^{-1} \cdot (d\gamma/d(\log[\text{surfactant}]) \quad (1)$$

The smaller this value with respect to the cross section of the hydrocarbon chain, the better the surfactants can pack in the monolayer at the air-water interface and the more water can be eliminated from the surface.[22] For each series of carbohydrate-derived surfactants, the area is significantly lower for the C_{12} derivative than for the C_8 derivative. Further addition of methylene groups into the alkyl chain increases their mutual attraction in the monolayer. Consequently, the density of the monolayer is increased, thereby reducing A_0. This result is in contrast with the results obtained by Boullanger *et al.*[14] who found A_0 for alkyl 2-amino-2-

deoxy-β-D-glucopyranosides equal to ~50 Å² irrespective of the chain length (C_8-C_{12}), indicating that the packing at the interface is controlled solely by interactions between the headgroups (hydrogen bonding).

Table 4. Areas (Å²) per surfactant molecule at the air-water interface of the carbohydrate-derived surfactants at 40°C.

	glucose	glucitol	lactose	lactitol
NC_2nC_8	56	55	68	64
NC_2nC_{10}	51	48	55	54
NC_2nC_{12}	38	35	57	55
NC_3nC_8	48	56	67	57
NC_3nC_{10}	48	52	57	59
NC_3nC_{12}	38	36	54	49

The areas at the air-water interface are similar for the surfactants having an acetyl or a propionyl substituent.

Based on our calculations, acylated disaccharide-derived surfactants containing eight carbon atoms in the alkyl chain possess large areas at the air water interface. The nonionic ethoxylated surfactants $C_{10}EO_8$ and $C_{12}EO_8$ also have large A_o values (66 and 59 Å², respectively, at 40°C).[23] Probably, the relatively large hydrated hydrophilic part prevents a close packing at the air-water interface.

A clear correlation exists between the area per surfactant molecule at the air-water interface and the surface tension at the CMC - the closer the packing at the surface, the lower γ_{CMC}. Disaccharide-derived surfactants have a large A_o, and consequently also a high γ_{CMC}.[24] Soderberg et *al.*[5] found that A_o increases with sequential addition of galactose structural units to the headgroup of carbohydrate-derivedsurfactants (sucrose < raffinose < stachyose).

In some cases, the area of the headgroups per molecule at the water-air interface (A_m) can be used as a rough estimation for a, in order to predict the micellar structure.[5] In our case, however, this procedure is not successful. Based on A_m, spherical micelles are predicted only for NC_2nC_8 lactose, NC_3nC_8 lactose, and NC_2nC_8 lactitol. This pattern disagrees with the predictions based on the mesophases formed by the surfactants.

3.4 Titration microcalorimetry

Standard enthalpies of micellization ($\Delta_{mic}H°$), Gibbs energies of micellization ($\Delta_{mic}G°$), and entropies of micellization ($\Delta_{mic}S°$), are important in understanding micelle formation in

aqueous solutions. In principle, the enthalpy of micellization for a given surfactant can be determined from the temperature dependence of the CMC. But this method has a major drawback, because $\Delta_{mic}H°$ is often significantly temperature dependent.[25,26] Enthalpies of micellization can be obtained accurately using modem, ultrasensitive titration microcalorimeters. With this technique the CMC is obtained and $\Delta_{mic}H°$ can often be read directly from a plot of the enthalpy of dilution *vs* the concentration.

3.4.1 Description of a microcalorimetric experiment

In a microcalorimetric experiment, a concentrated micellar solution (5-10 μL, concentration >> CMC) is injected into the sample cell which initially contains water. As the concentration of the surfactant in the sample cell is below the CMC of the surfactant, the micelles deaggregate upon injection. The accompanying heat is recorded by the microcalorimeter. The next aliquot of surfactant solution is injected when the system has reached thermal equilibrium. A typical titration plot is shown in Figure 3. The process takes place at constant pressure, an so the heat recorded in the titration experiment is equal to the change in enthalpy. Figure 4 shows the integrated plot, the enthalpy of dilution vs the injection

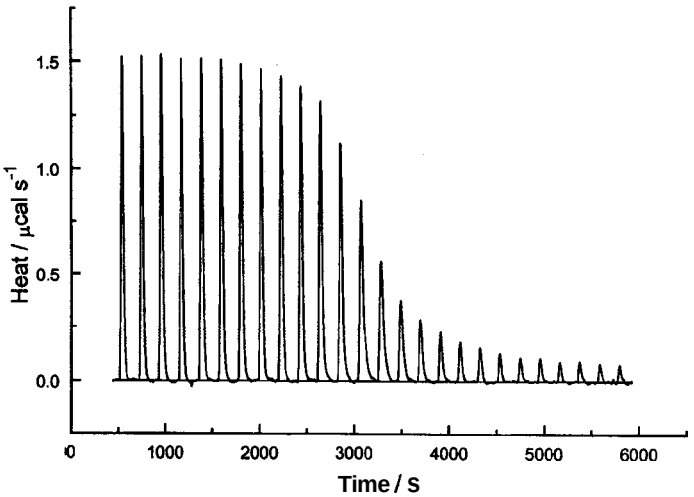

Figure 3. Calorimetric signals corresponding to dilution of a concentrated solution of NC_2nC_{12}lactitol at 40°C.

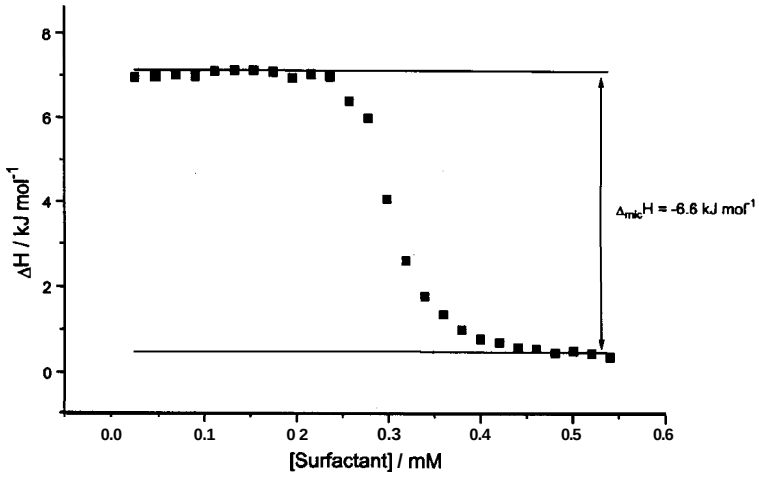

Figure 4. Enthalpy of dilution of NC_2nC_{12} lactitol at 40°C.

number. The enthalpogram obtained is a step-shaped plot identifying two concentration regions where the recorded heats per mole of injected surfactant are almost constant.'' In the low concentration region, the recorded heats are due to deaggregation and dilution of the monomers. As already explained, the surfactant concentration in the sample cell is below the

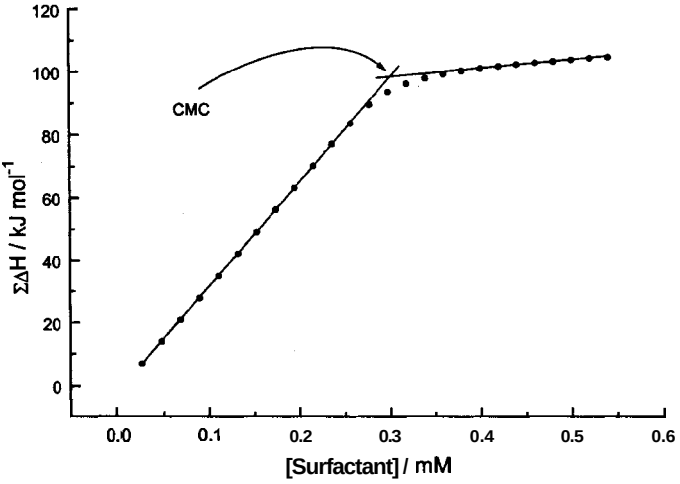

Figure 5. Cumulative enthalpy of dilution of NC_2nC_{12} lactitol vs concentration at 40°C: determination of the CMC.

CMC and the micelles of the injected aliquots deaggregate. The large change in the recorded heat (in this particular case a decrease) over a small concentration range indicates that the CMC in the sample cell has been exceeded. Upon further additions of aliquots, the micelles in the injected micellar solution do not deaggregate and the recorded heat in the high concentration region can mainly be attributed to dilution of micelles. The enthalpy of micellization is the difference in recorded heat per mole of injected surfactant between the two horizontal parts of the step-shaped curve.

The CMC is obtained from a so-called van Os plot of the cumulative heats per mole of injected surfactant *vs* the concentration of surfactant in the sample cell (Fig. 5).[28-30]

3.4.2 Standard Gibbs energies and entropies of micellization

We used the phase equilibrium model to calculate the standard Gibbs energies and entropies of micellization (mole fraction scale).[31] According to the phase equilibrium model, the micelles in the system constitute a separate phase. The monomers are solutes in aqueous solution which are assumed to have ideal properties. Then for micelles in the micellar phase, at a fixed temperature and pressure, the chemical potential is denoted as:

$$(\text{chemical potential of micelles in the micellar phase})_{,,} = \mu^*(X_{,};\ \text{micellar}) \qquad (2)$$

Herein, X_N indicates the micellar phase with aggregation number N. The superscript * indicates a ***pure*** phase.

In the aqueous phase, there are monomers X(aq) which are assumed to have ideal properties. The chemical potential of the monomers expressed in the mole fraction scale[b] is given by equation **(3):**

$$\mu_x(aq) = \mu_x^\circ(aq) + RT \ln (x_x) \qquad (3)$$

Where x_x is the mole fraction of solute X and $\mu_x^\circ(aq)$ is the chemical potential of ***solute*** X in a ***solution*** when the mole fraction of aqueous X is ***one.***

Surfactant monomers can go from one phase to the other: $X_N \rightleftharpoons N \cdot X(aq)$. At equilibrium, the potentials are balanced:

$$\mu^*(X_{,};\ \text{micellar}) = N\,[\mu^\circ_x(aq) + RT \ln (x_x)] \qquad (4)$$

---

[b] The chemical potential of the surfactant in solution can also be expressed in a molar scale or in a molality scale?'

Divided by N:

$$\mu^*(X; \text{micellar}) \cdot N^{-1} = [\mu^\circ_x(aq) + RT \ln(x_x)] \quad (5)$$

By definition:

$$\Delta_{mic}G^\circ = [p^*(X_N; \text{micellar}) \cdot N^{-1}] - \mu^\circ_x(aq) \quad (6)$$

thus:

$$\Delta_{mic}G^\circ = RT \ln(x,) \quad (7)$$

In words, $A_{mic}G^o$ is the change in standard potential for one mole of monomer passing from the aqueous solution into the micellar phase formed by N monomers. Furthermore, the mole fraction x_x is:

$$x_x = n_x \cdot (n, + n_1)^{-1} \quad (8)$$

Herein, n, is the amount of water and n_x the amount of surfactant in the aqueous surfactant solution. For dilute solutions, $n_x + n, \simeq n,$, thus:

$$x_x = n_x \cdot n_1^{-1} = (n, \cdot V^{-1}) \cdot (V \cdot n_1^{-1}) = CMC \cdot (V \cdot n_1^{-1}) \quad (9)$$

Where V is the volume of the system, which is approximately the volume of pure water in the ideal solution and consequently, $(V \cdot n_1^{-1})$ is approximately the molar volume of water, which is 55.08 rnol L^{-1} at 40 °C. The amount of monomers per volume is equal to the CMC of the surfactant. Thus the equation by which the standard Gibbs energies of micellization are calculated is given by (10):[32]

$$\Delta_{mic}G^\circ = RT \ln(CMC / 55.08) \quad (10)$$

The advantage of nonionic surfactants over ionic surfactants is that equation (10) can be used without the necessity to take into account the degree of counterion binding. For ionic surfactants, the extent of counterion binding has to be estimated[3] and as a result, equation (10) is more complicated and less accurate.

The standard entropy of micelle formation per mole of monomer is calculated from:

$$\Delta_{mic}S^\circ = (\Delta_{mic}H^\circ - \Delta_{mic}G^\circ) / T \quad (11)$$

In general, the entropy term provides the main driving force for micelle formation by nonionic surfactants.[28,33-36] As micelles are formed, the hydrophobic hydration layers around the alkyl chains are broken down (Chapter 1). This process is accompanied by a gain in entropy and represents the driving force for hydrophobic interactions within micelles. The nature of this hydrophobic effect has been discussed in detail.[37]

3.4.3 CMCs determined by titration microcalorimetry

Table 5 shows the experimental data obtained using titration microcalorimetry. The critical micelle concentrations are similar to the CMCs determined by drop tensiometry. The small discrepancies in the values obtained by the two different methods do not show a consistent trend, *i.e.*, one method does not always yield lower values than the other.

CMCs of surfactants with the same headgroup but with alkyl chains longer than C_{12} cannot be measured by drop tensiometry, due to the very low surfactant concentrations that need to be used. The migration of surfactant monomers to the expanding surface during drop formation disturbs the measurements. The sensitivity of the titration microcalorimeter is primarily determined by the magnitude of the enthalpy of micellization and by possible nonideality of the solutions.[27] $\Delta_{mic}H^{\circ}$ increases with increasing chain length and nonideality is only observed when the CMCs measured are high. Thus CMCs of chain analogs with an alkyl chain containing more than 12 carbon atoms can be measured by microcalorimetry.

3.4.4 Enthalpy of micellization obtained by titration microcalorimetry

Standard enthalpies of micellization were obtained directly from the enthalpograms (Table 5, $\Delta_{mic}H^{\circ}$ experimental). Surfactants with a decyl or dodecyl chain produced enthalpograms conforming to the text-book case in which the heats per mole of injected surfactant were constant over the two ranges, above and below the CMC, in the sample cell. But for octyl-chain analogs there was a slow increase in the injected heats in the premicellar region, indicating a concentration-dependent change in interactions. This slope is accounted for in terms of non-ideal thermodynamic properties of the solutions in both the syringe and the sample cell and reflects micelle-micelle, monomer-monomer, and monomer-micelle interactions.[27,38] This feature was especially pronounced for the C_8 surfactants because, as a consequence of high CMC, the concentration of surfactant in the syringe was high.[27,28]

Table 5. CMCs and thermodynamic parameters of rnicellization of glucose-, glucitol-, lactose-, and lactitol-derived surfactants at 40°C.

Compound	CMC (mM)	$\Delta_{mic}H°$ (kJ mol^{-1}) experimental	$\Delta_{mic}H°$ (kJ mol^{-1}) calculated	$\Delta_{mic}G°$ (kJ mol^{-1})	$T\Delta_{mic}S°$ (kJ mol^{-1})
NC_2nC_8 glucose	21	endothermic	+1.4	-20.5	21.9
NC_2nC_{10} glucose	2.9	-3.0	-2.9	-25.6	22.7
NC_2nC_{12} glucose	0.26	-7.7	-7.5	-31.9	24.4
NC_3nC_8 glucose	20	- +2.7	+3.4	-20.6	24.0
NC_3nC_{10} glucose	1.8	-1.3	-1.3	-26.9	25.6
NC_3nC_{12} glucose	0.19	-5.4	-5.7	-32.8	27.1
NC_2nC_8 glucitol	21	> +0.9	+1.7	-20.5	22.2
NC_2nC_{10} glucitol	2.0	-2.6	-2.5	-26.6	24.1
NC_2nC_{12} glucitol	0.18	-7.2	-7.0	-32.9	26.0
NC_3nC_8 glucitol	13	≥ +2.6	+3.0	-21.8	24.7
NC_3nC_{10} glucitol	1.2	-1.9	-1.8	-27.9	26.1
NC_3nC_{12} glucitol	0.11	-7.2	-7.2	-34.3	27.1
NC_2nC_8 lactose	35	+2.0	+4.3	-19.2	23.5
NC_2nC_{10} lactose	4.6	-1.4	-1.2	-24.4	23.2
NC_2nC_{12} lactose	0.45	-5.3	-5.3	-30.5	25.2
NC_3nC_8 lactose	24	+5.0	+7.5	-20.1	27.6
NC_3nC_{10} lactose	2.6	+0.1	0	-25.9	25.9
NC_3nC_{12} lactose	0.31	-4.1	-4.0	-31.5	27.5
NC_2nC_8 lactitol	24	>+1.1	+2.3	-20.2	22.5
NC_2nC_{10} lactitol	3.3	-1.9	-1.9	-25.3	23.5
NC_2nC_{12} lactitol	0.31	-6.6	-6.5	-31.5	25.0
NC_3nC_8 lactitol	18	> +2.3	+2.9	-20.8	23.7
NC_3nC_{10} lactitol	1.8	-1.5	-1.4	-26.9	25.5
NC_3nC_{12} lactitol	0.16	-6.1	-6.2	-33.1	26.9

Therefore, these enthalpograms were fitted using an iterative procedure incorporated into a Turbo-Basic program. The equations describing deaggregation of the rnicelles took account of the non-ideal properties of the solution in both sample cell and injected aliquots using

enthalpic pairwise interaction parameters involving rnicelles and monomers in the aqueous solutions. The aggregation number for the micelles was set at 50.[19,39] The enthalpies of rnicellization obtained via the program did not depend on the aggregation number. The remaining variable was the standard enthalpy of micelle formation. Satisfactory agreements were obtained between calculated and observed enthalpograms. The calculation and the method were supported by the results which produced enthalpies of rnicelle formation which conformed to the pattern observed for the C_{10} and C_{12} surfactants.

Figures 6 and 7 show the experimental and fitted enthalpograms of NC_2nC_{12} lactitol and NC_2nC_8 glucitol. Enthalpies obtained using the computer program, are listed in Table 5.
There are two contributions to $\Delta_{mic}H°$: (i) an endothermic contribution from headgroup interactions and (ii) an exothermic contribution from alkyl chain packing.[36,40-42] For alkylpolyethyleneglycol ethers the magnitude of the endothermic contribution of the headgroups depends on the extent to which water is liberated into the bulk solvent upon micellization. As the degree of ethoxylation increases, the hydration and $\Delta_{mic}H°$ increase correspondingly. Disaccharide derivatives have more hydroxyl groups and show an increase in $\Delta_{mic}H°$ (*i.e.* more endothermic) relative to their monosaccharide counterparts.

On going from C_8 to C_{12} the exothermic contribution of the alkyl chain increases, whereas the endothermic contribution of the headgroup remains constant and, therefore, the enthalpy of micellization becomes more favorable. Hence, $\Delta_{mic}H°$ changes from endothermic to exothermic. It is possible that for a given surfactant at a certain temperature, the endothermic contribution of the headgroup and the exothermic contribution of the chain cancel out and, consequently, $\Delta_{mic}H°$ equals zero. The temperature at which $\Delta_{mic}H° = 0$ may be called the transition temperature. According to Table 5 NC_3nC_{10} lactose has a transition temperature of 40°C. The transition temperature at which $A_{\mu}H^{o}$ changes sign from positive to negative is lower for analogs with longer alkyl chains.'' Therefore it is not surprising that at 40°C the analogs with a C_8 chain are below and the C_{12} analogs are above the transition temperature.[28,43]

The contribution of each methylene group to the enthalpy of micellization for each series, $A_{mic}H^{o}$ (CH_2), is approximately -2.4 kJ mol^{-1} (Table 6). This pattern is in good agreement with increments reported for other surfactants.[11,42,44-46] In our case, the $\Delta_{mic}H°$ (CH_2) are self-consistent and do not show large deviations from the average value.

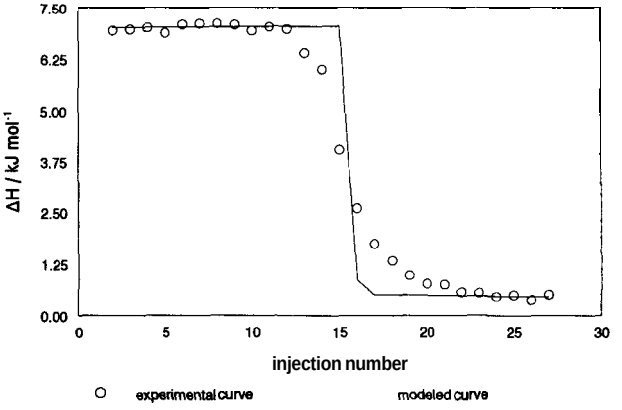

Figure 6. Experimental and fitted enthalpograms of NC_2nC_{12} lactitol.

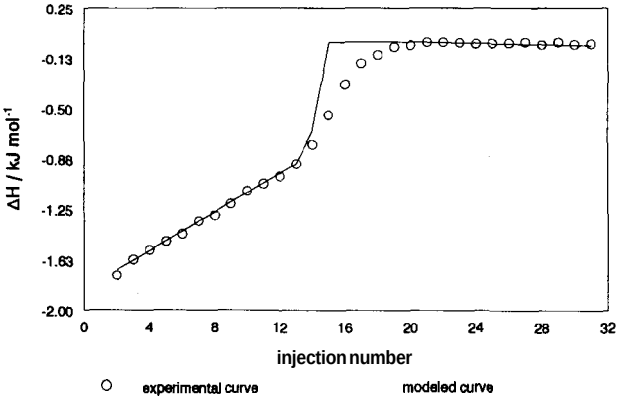

Figure 7. Experimental and fitted enthalpograms of NC_2nC_8 glucitol.

Table 6. Contributions of a CH, group to $\Delta_{mic}H°$, $\Delta_{mic}G°$, and $T\Delta_{mic}S°$ at 40°C for a series of glucose-, glucitol-, lactose-, and lactitol-derived surfactants.

Compound	$\Delta_{mic}H°$ per CH, (kJ mol^{-1})	$\Delta_{mic}G°$ per CH, (kJ mol^{-1})	$T\Delta_{mic}S°$ per CH, (kJ mol^{-1})
NC_2nC_n glucose	-2.2	-2.9*	0.6*
NC_3nC_n glucose	-2.3	-3.1	0.8
NC_2nC_n glucitol	-2.2	-3.1	0.9
NC_3nC_n glucitol	-2.5	-3.1	0.6*
NC_2nC_n lactose	-2.4*	-2.8	0.4‡
NC_3nC_n lactose	-2.8*	-2.8	[b]
NC_2nC_n lactitol	-2.2	-2.8	0.6
NC_3nC_n lactitol	-2.3	-3.1	0.8

[a] The regression constant exceeds 0.999, except for the results marked with * (0.98-0.99) and ‡ (0.81). [b] The value of $T\Delta_{mic}S°$ for NC_3nC_8 lactose deviates from the general trend. Therefore, $T\Delta_{mic}S°$ per CH, for this series was not calculated.

3.4.5 Gibbs energy and entropy of micellization obtained by titration microcalorimetry

All estimates of $\Delta_{mic}G°$ are negative, their absolute values increase with increasing chain length. The contribution of each CH, group to $\Delta_{mic}G°$ is -3.0 kJ mol^{-1}.[5,11,12,14,33,41,42,46-50] This is slightly lower than the standard Gibbs energy of transfer per CH, of n-alkanes from water to pure liquid, because the environment of a given CH_2 group in the interior of a micelle differs from that in the pure liquid.[33,35,50,51]

The entropy terms ($TA_{mic}S^{o}$) are positive and increase with increasing chain length. Estimates of $T\Delta_{mic}S°$ are large compared with those for ionic surfactants. The hydrophobic hydration of alkyl chains belonging to ionic surfactants is probably less than for nonionic surfactants, due to the strongly hydrated headgroups of the anionic surfactants. Consequently, the amount of entropy gained upon micellization is less for the anionic surfactants.[34,35,36] $TA_{mic}S^{o}$ per CH, is c. 0.7 kJ mol^{-1}. The main driving force for micellization at 40°C is provided by the entropy term, supported in some cases by an exothermic enthalpy term.

3.4.6 The effect of variations in the carbohydrate-derived surfactants on the standard Gibbs energies of micellization

When the length of the alkyl chain is increased, the standard Gibbs energy of micellization becomes more favorable by 3.0 kJ mol" per CH_2. Surprisingly, this is mainly due to the decrease in ***enthalpy*** of micelle formation. Thus, although $\Delta_{mic}S°$ is the driving force for the micelle formation by surfactants with short chain lengths, the ***enthalpy*** change predominates for CH_2 increments as the length of the chain is increased. This pattern has also been observed for other surfactants and alcohols with long chains and has been accounted for by a degree of backfolding of the chains.[35]

Changing the acyl group from acetyl to propionyl leads to a more favorable standard Gibbs energy of micellization. This pattern is dominated by the ***entropy*** change and finds its origin in the increase in the hydrophobic character of the surfactant. Consequently, the hydrophobic hydration shell is larger and more entropy is gained when the monomers aggregate to form micelles. The CH, of the propionyl group is too small to give the effect of backfolding.

As mentioned earlier, a lactose-derived headgroup is less favorable for micelle formation compared to a glucose-derived headgroup. An increase in the number of hydroxyl groups increases the endothermic contribution to the enthalpy of micellization and renders the change in Gibbs energy less favorable.

An alditol headgroup is more favorable for micelle formation than an aldose headgroup. This pattern is mainly caused by the changes in the enthalpy term and indicates that the hydration layers of the reduced carbohydrate headgroups are smaller.

Consequently, NC_3nC_{12} glucitol exhibits the most favorable standard Gibbs energy of micellization and forms the most stable micelles.

3.5 Conclusions

Judging from their lyotropic liquid-crystalline behavior, the monosaccharide-derived surfactants and the propionylated disaccharide-derived surfactants form cylindrical micelles. The acetylated disaccharide-derived surfactants appear to form spherical micelles.

The disaccharide-derived surfactants show higher surface tensions at the CMC and larger areas per surfactant molecule at the air-water interface. Increasing alkyl chain lengths leads to lower γ_{CMC} values and smaller headgroup areas at the air-water interface.

The carbohydrate-derived surfactants show CMCs, standard enthalpies, standard Gibbs energies and standard entropies of micellization which are linear functions of alkyl chain length, indicating equivalence with respect to micelle formation of the methylene groups at least beyond C_7. The decrease in CMC is tenfold when the chain length is increased by two

methylene groups. The contribution of an additional CH_2 group to $\Delta_{mic}H°$, $\Delta_{mic}G°$, and $T\Delta_{mic}S^o$ at 40 °C is -2.4 kJ mol^{-1}, -3.0 kJ mol^{-1}, and 0.7 kJ mol^{-1} respectively. The consistency of the increments per rnethylene group of $\Delta_{mic}H°$, $A_{mic}G^o$, and $T\Delta_{mic}S^o$ sheds important light on the "hydrophobic " component in rnicelle formation of nonionic amphiphiles. The more favorable standard Gibbs energies (and the lower CMCs) for the longer chain analogs are caused predominantly by an exothermic shift in the enthalpy of rnicelle formation.

3.6 Experimental

Drop tensiometry. Critical micelle concentrations were determined with a TVT 1 Lauda drop tensiometer. Doubly distilled water was used. The determination of a CMC covered 15 measurements in the concentration range of roughly 0.1 . CMC to 10 . CMC. The measured surface tension is the mean value of 4 - 5 drop cycles.

Titration microcalorimetry. A Microcal Omega titration microcalorimeter (Microcal, Northampton, MA, USA) was used. Water was doubly distilled and all solutions were degassed before use. The solution in the sample cell was thermostatted at 40 °C, and stirred (350 rpm). An aqueous surfactant solution (5-10 μL, concentration >> CMC) was injected under computer control into the sample cell, which initially contained 1.3 mL of water. The heat absorbed or evolved was recorded and after thermal equilibrium was reached, the next aliquot of 5-10 μL was injected. This procedure was repeated until the concentration of surfactant in the sample cell was well above the CMC. The crude data (Figure 3) were analyzed using Omega software (Origin 2.9), yielding a plot of the enthalpy of dilution against surfactant concentration in the cell, the enthalpogram (Figure 4).[28,29,30]

Calculated enthalpies of micellization. The experimental enthalpograms were fitted using an iterative procedure incorporated into a Turbo-Basic program. Three variable interaction terms (a monomer-monomer interaction term, a monomer-micelle interaction term and a micelle-micelle interaction term) were introduced and accounted for the slopes of the step-shaped plot. The CMC indicated the turning point and, finally, an estimate for the enthalpy of micellization gave the right distance between the "horizontal" lines before and after the point at which the CMC had been reached. The fit was only reliable if initial estimates of the enthalpy of micellization were close to the final value.

Acknowledgements. Jan Kevelam (Department of Organic and Molecular Inorganic Chemistry, University of Groningen) kindly performed the microcalorimetric experiments. We sincerely thank Prof. Mike Blandamer (University of Leicester, U.K.) for the lively discussions on the thermodynamic aspects and for developing the Turbo-Basic program. We also thank Jan Hoen (HLO trainee, Netherlands Institute for Carbohydrate Research, Groningen) for calculating confidence intervals of

CMCs measured using drop tensiometry.

3.7 References

Bleasdale, T. A.; Tiddy, G. J. T. In *The Structure, Dynamics and Equilibrium Properties of Colloidal Systems;* Bloor, D. M., Wyn-Jones, E., Eds; Kluwer Academic Publishers: The Netherlands, 1990; p. 397.

2. Seddon, J. M.; Templer, R. H. *Phil. Trans.* R. *Soc. Lond. A* 1993,344,377.

3. Israelachvili, J. N. *Intermolecular and Surface Forces;* Academic Press: London, *U.K.* 1996; p. 366.

4. Israelachvili, J. N.; Mitchell, D. J.; Ninham, B. W. *J. Chem. Soc., Faraday Trans* 2 1976, 72, 1525.

5. Soderberg I.; Drummond, C. J.; Furlong, D. N.; Godkin, S.; Matthews, B. *Coll Surf., A: Physicochem. Eng. Aspects* 1995, *102*, 91.

6. Nilsson, F.; Söderman, O. *Langmuir* 1996, *12*, 902.

7. Van Doren, H. A.; Terpstra, K. R. *J. Mater. Chem.* 1995, *5*, 2153.

8. Van Doren, H. A. In *Carbohydrates* as *Organic Raw Materials III*; van Bekkum, *H.,* Roper, H., Voragen, A. G. J., Eds; VCH Publishers: Weinheim, Germany, 1996; p. 255.

9. Auray, X; Pepitas, C.; Anthore, R.; Rico-Lattes, I.; Lattes, A. *Langmuir* 1995, 11,433.

10. Van Os, N.M.; Haak, J. R.; Rupert, L. A. M. In *Physico-chemical Properties of Selected Anionic, Cationic and Nonionic Surfactants*; Elsevier: Amsterdam, The Netherlands, 1993.

Okawauchi, M.; Hagio, M.; Ikawa, Y.; Sugihara, G.; Murata, Y.; Tanaka, M. *Bull. Chem. Soc. Jpn.* 1987, *60*, 2718.

12. Kratzat, *K.;* Finkelmann, H. *Langmuir* 1996, *12*, 1765.

13. Hayes, M. E.; El-Emary, M.; Schechter, R. S.; Wade, W. H. *J. Disp. Sci. Technol.* 1980, *1*, 297.

14. Boullanger, P.; Chevalier, Y. *Langmuir* 1996, *12*, 1771.

15. Retailleau, L.; Laplace, A.; Fensterbank, H.; Larpent, C. *J. Org. Chem.* 1998, *63, 608.*

16. Van Doren, H. A. In *Starch 96, The Book;* van Doren, *H.* A.; Van Swaaij, A. C., Eds; The Carbohydrate Research Foundation, Zestec: The Hague, The Netherlands, 1997; p. 123.

17. Straathof, A. J. J., *Carbohydrates in The Netherlands* 1988.4, 27.

18. Costes, F.; El Ghoul, M.; Bon, M.; Rico-Lattes, I.; Lattes, A. *Langmuir* 1995, 11,3644.

19. Rico-Lattes, I.; Lattes, A. *Coll. Surf., A: Physicochem. Eng. Aspects* 1997, *123-124*, 37.

20. Evans, D. F.; Wennerström, H. *The Colloidal Domain, Where Physics, Chemistry, Biology, and Technology Meet;* VCH Publishers: New York, U. S. A., 1994; p. 68.

21. Van Buuren, A. R.; Berendsen, H. J. C. *Langmuir* 1994, *10*, 1703.

22. Hoffmann, H. *Progr. Colloid Polym. Sci.* 1990, *83*, 16.

23. Arai, T.; Takasugi, *K.;* Esumi, K. *Coll. Surf., A: Physicochem. Eng. Aspects* 1996, *119*, 81.

24. Kida, T.; Yurugi, *K.;* Masuyama, A.; Nakatsuji, Y.; Ono, D.; Takeda, T. *J. Am. Chem. Oil Soc.* 1995, 72,773.

25. Kresheck, G. C.; Hargraves, W. A. *J. Colloid Interface Sci.* 1974, *48*, 481.

26. Olofsson, *G. J. Phys. Chem.* 1983, *87*, 4000.

27. Bijma, K. *Surfactant Structure and Thermodynamics of Micelle Formation,* Ph. D. Thesis, University of Groningen, The Netherlands, **1995.**

28. Paula, S.; Süs, W.; Tuchtcnhagen, J.; Blume, A. *J. Phys. Chem.* **1995,** *99, 11742.*

29. Király, Z.; Bomer, R. H. K.; Findenegg, G. H. *Langmuir* **1997**, *13*, **3308.**

30. Heerklotz, H.; Lantzsch, G.; Binder, H.; Klose, G.; Blume, A. J. *Phys. Chern.* **1996,100,6764.**

31. Blandamer, M. J.; Cullis, P. M.; Soldi, L. G.; Engberts, J. B. F. N.; Kacperska, A.; van Os, N. M.; Subha, M. C. S. *Adv. Coll. Int. Sci.* **1995**, *58*, **171.**

32. Molyneux, P.; Rhodes, C. T.; Swarbrick, *Trans. Faraday Soc.* **1965**, *61*, **1043.**

33. Clint, J. H.; Walker, T.; *Trans. Faraday Soc.* **1975, 71,946.**

34. Jolicœur, C.; Philip, P. R. *Can. J. Chem.* **1974**, *52*, **1834.**

35. Benjamin, L. *J. Phys. Chem.* **1964**, *68*, 3575.

36. Förster, Th; von Rybinski, W. *Tenside Surf: Det.* **1990**, *27*, 254.

37. Blokzijl, W.; Engberts, J. B. F. N. *Angew. Chem., Int. Ed. Engl.* **1993,** *32,* 1545

38. Blandamer, M. J.; Cullis, P. M.; Engberts, J. B. F. N. *J. Thermal Anal.* **1995**, *45*, 599.

39. Dupuy, C.; Auvray, X.; Petipas, C.; Anthore, R.; Costes, F.; Rico-Lattes, I.; Lattes, A. *Langmuir* **1996**, *12*, 3162.

40. Moroi, *Y.*; Nishikido, N.; Uehara, H.; Matuura, R. *J. Coll. Int. Sci.* **1975, 50, 254.**

41. Corkill, J. M.; Goodman, J. F.; Tate, J. R. *Hydrogen-Bonded Solvent Systems, Proc. Symp.* **1968, 181.**

42. Mehrian, T.; de Keizer, A.; Korteweg, A. J.; Lyklema J. *J. Coll. Surf, A: Physicochem., Eng. Aspects* **1993, 71,255.**

43. Fisicaro, E.; Barbieri, M.; Pelizzetti, E.; Savarino, P. *J. Chem. Soc., Faraday Trans.* **1991**, *87*, **2983.**

44. Bijma, K.; Engberts, J. B. F. N.; Haandrikman, G.; van Os, N. M.; Blandamer, M. J.; Butt, M. D.; Cullis, P. M. *Langmuir* **1994, 10, 2578.**

45. Różycka-Roszak, B.; Fisicaro, E. *J. Colloid Interface Sci.* **1993, 159, 335.**

46. Corkill, J. M.; Goodman, J. F.; Tate, J. R. *Trans Faraday Soc.* **1964**, 60, **996.**

47. Andersson, B.; Olofsson, G. *J. Chem. Soc., Faraday Trans. I* **1988**, *84*, 4087

48. Zajac, J.; Chorro, C.; Lindheimer, M.; Partyka, S. *Langmuir* **1997, 13,** *1486.*

49. Sokolowski, A.; Burczyk, B.; Beger, J. *Abh. Akad. Wiss. DDR, Abt. Math. Naturwiss. Tech.* **1986,** *1N,* 419; *Chem. Abstr.* **1988,108,2066995.**

50. Némethy, G.; Scheraga, H. A. *J. Chem. Phys.* **1962**, *36*, 3401.

51. Nelson, H. D.; De Ligny, C. L. *Recl. Trav. Chim. Pays-Bus* **1968.87, 528.**